



**A center of excellence in earth sciences and engineering®**

Geosciences and Engineering Division  
6220 Culebra Road • San Antonio, Texas, U.S.A. 78238-5166  
(210) 522-5160 • Fax (210) 522-5155

August 5, 2016  
Contract No. NRC-HQ-50-14-E-0001  
Task Order No. NRC-HQ-25-15-T-0001(49)  
Account No. 20.19941

U.S. Nuclear Regulatory Commission  
ATTN: Mr. Gerry Stirewalt  
NRO/DSEA/RGS2  
Mail Stop: TWFN 7-F18  
Rockville, Maryland 20852

Subject: AI 19941.01.001.100: Task 1a(i): Diablo Canyon—Technical Assessment of Applicant Data

Dear Mr. Stirewalt:

This letter documents transmittal of a technical report, in accordance with the subject deliverable. We developed the report to document, in part, our technical assessment of the Pacific Gas & Electric (PG&E) seismic data with regard to the Diablo Canyon Power Plant (DCPP). Based on discussions with the U.S. Nuclear Regulatory Commission (NRC) technical team, and you as Contracting Officer Representative, we focused this report on the potential slip rates of the Hosgri fault because this parameter was deemed by the Diablo Review Team to be the most significant contributor to the Seismic Source Characterization model. Uncertainty in the slip rate on the Hosgri fault has a direct impact on the level of the resulting hazard at the DCPP. Our team will continue to provide support to the NRC staff in developing the Staff Assessment for the DCPP hazard re-evaluation, and this support will be documented in later deliverables in accordance with the milestone schedule.

Please contact Ronald McGinnis at 210.522.5825, Dr. John Stamatakos at 301.881.0290, or me at 210.522.3266 if you have questions concerning this subject deliverable.

Sincerely,

Miriam Juckett  
Program Manager  
Environmental Protection and  
External Hazards Assessment

MJ/ar  
G:\EWC - 19941 WUS\Deliverables\19941.01.001.100

cc: NRC	GED/CNWRA
Meralis Plaza-Toledo	CNWRA Correspondence
Jon Ake	Miriam Juckett
Clifford Munson	John Stamatakos
Sharlene McCubbin	



Washington Office  
1801 Rockville Pike, Suite 105 • Rockville, Maryland 20852-1633

**INDEPENDENT EVALUATION OF THE HOSGRI FAULT  
SLIP RATE BASED ON A STRUCTURAL ANALYSIS OF  
THE PULL-APART BASIN LINKING THE HOSGRI AND  
SAN SIMEON FAULT SYSTEMS**

*Prepared for*

**U.S. Nuclear Regulatory Commission  
Contract No. NRC-HQ-50-14-E-0001**

*Prepared by*

**Ronald N. McGinnis  
Alan P. Morris  
David A. Ferrill  
Kevin J. Smart  
John A. Stamatakos  
Miriam R. Juckett**

**Center for Nuclear Waste Regulatory Analyses  
San Antonio, Texas**

**August 2016**

# TABLE OF CONTENTS

Section	Page
FIGURES .....	iii
TABLES .....	iv
EXECUTIVE SUMMARY .....	v
ACKNOWLEDGMENTS .....	vii
1 INTRODUCTION.....	1-1
1.1 Background .....	1-1
1.2 Purpose .....	1-3
1.3 Scope .....	1-3
2 ANALYSIS.....	2-1
2.1 Seismotectonic Setting .....	2-1
2.2 Transensional Features Along the Hosgri Fault .....	2-2
2.3 Methodology .....	2-8
2.4 Dip-Slip Versus Oblique-Slip on the Half Graben Fault.....	2-11
2.5 Uncertainty in Slip Rate .....	2-12
3 RESULTS.....	3-1
4 DISCUSSION .....	4-10
5 CONCLUSIONS .....	5-1
6 REFERENCES.....	6-1

## FIGURES

Figures	Page
1-1 Regional Location Map .....	1-2
2-1 Map of the Study Area .....	2-6
2-2 (A) Map View of the Principal Geometric Elements of the Hosgri and Half Graben Faults, and Illustrating How the Magnitude of Hosgri-Parallel Slip Is Independent of the Direction of Slip on the Half Graben Fault. (B) Map View Similar to (A) Showing the Nature and Magnitude of Error Introduced by Assuming that the Seismic Section Trace in Which the Half Graben Heave Is Measured Is Perpendicular to the Half Graben Fault Trace.....	2-7
2-3 COMAP Seismic Reflection Example .....	2-8
2-4 High-Resolution Sparker Tracklines (PBS) Seismic Reflection Example.....	2-9
3-1 Half Graben Fault Vector Map for All Seismic Lines That Were Evaluated in This Analysis .....	3-5
3-2 Plot Showing Slip Rate for Each Seismic Line and Each Unconformity Versus Distance Along Half Graben Fault Trace With Respect to the Southernmost Line Used in This Analysis.....	3-7
3-3 Calculated Horizontal Slip Rate for the Hosgri Fault Over Time .....	3-8
3-4. Plot of Slip Rates Versus Age .....	3-9

## TABLES

Tables	Page
2-1 Hosgri Fault Slip Rates From Published Sources .....	2-4
2-2 Possible Error in the Half Graben Fault Analysis Arising From Nonideal Cross-Section Orientation .....	2-14
3-1 Results From Fault Analysis .....	3-2

## EXECUTIVE SUMMARY

All recent seismic source characterization studies conducted to assess the seismic hazards at the Diablo Canyon Power Plant have identified the Hosgri fault as the dominant seismic source. The Hosgri fault—a 160 km long, right-lateral (dextral) strike-slip fault—is located just a few kilometers offshore south-central California and generally parallels the central California coastline. Characterization of the fault is primarily based on submarine mapping from seismic reflection data. The Hosgri Fault has been the focus of considerable research since it was first identified as an important regional structure during hydrocarbon exploration in the 1970s that focused on the Santa Maria basin. However, beginning in the early 1980s and into the 1990s, the Pacific Gas and Electric Company (PG&E), in collaboration with the United States Geological Survey and academic research groups, began investigating the Hosgri fault as a potential seismic source that could affect the Diablo Canyon Power Plant. These investigations were conducted as part of the PG&E Long-Term Seismic Program.

In the recent probabilistic seismic hazard analyses (PSHA) developed for Diablo Canyon Power Plant, the Hosgri fault is recognized as the major contributor to the overall seismic hazard at the plant. The importance of the Hosgri fault is due to its close proximity to the site, the relatively large magnitude earthquakes that can be generated along the fault because of its 160 km length, and an order-of-magnitude higher earthquake recurrence interval compared to other nearby faults. Slip rate on the Hosgri fault is thus one of the most important parameters in these probabilistic seismic hazard studies. Results from the Long Term Seismic Program concluded that the Quaternary slip rates for the Hosgri Fault were 1–3 mm/yr. More recent studies of offshore data conducted over the past two decades, including those that were recently required by the State of California as part of the California Assembly Bill 1632, generally confirm these prior interpretations.

The most recent detailed technical assessment of the slip rate of the Hosgri fault was carried out by PG&E as part of the 2015 updated PSHA for the Diablo Canyon Power Plant (PG&E, 2015a,b). This updated PSHA was provided in response to the 2012 post-Fukushima information request from the U.S. Nuclear Regulatory Commission (NRC), pursuant to 10 CFR 50.54(f). The resulting PSHA showed that slip rate on the Hosgri fault is a major contributor to the overall seismic hazard at the plant and to the uncertainty in the resulting probabilistic ground motions. As a result, slip rate of the Hosgri fault is a critical parameter in the PSHA seismic source characterization model and has a nearly one-to-one relationship to probabilistic ground motion levels in the resulting PSHA hazard curves.

In the 2015 PSHA (PG&E, 2015a,b), PG&E analyzed or re-analyzed evidence of fault slip at four sites along the Hosgri fault. These analyses included analysis or re-analysis of (i) an offset marine terrace strandline near San Simeon (referred to as Oso Terrace), (ii) offset of the shoreface of a late Pleistocene sand spit between Morro Bay and Point San Simeon (referred to as the Cross-Hosgri slope), (iii) dextral separation of a buried paleo-channel in Estero Bay, and (iv) dextral separation of a buried paleo-channel near Point Sal. Median slip rates based on these four offset measurements and ages of the offset features ranged between 0.8 mm/yr (Point Sal) and 2.5 mm/yr (Cross-Hosgri slope), with a weighted mean from all four sites of 1.7 mm/yr  $\pm$  0.7 mm/yr (1 standard deviation).

Consistent with a risk-informed regulatory review, the focus of the NRC staff's evaluation of the PG&E PSHA (PG&E, 2015a,b) is an assessment of all the available information that can be used to justify and constrain slip rate estimates for the Hosgri fault. As part of this review, a half-graben that formed where displacement on the Hosgri fault appears to be transferring its

slip to the San Simeon fault along a right-stepping extensional pull apart was identified and studied because growth of this pull-apart provides an independent estimate of the Hosgri fault slip rate. This half graben and associated extensional fault zone is situated a few kilometers offshore, 23 to 40 km northwest of the Diablo Canyon Power Plant. As the pull-apart developed, sediments accumulated along the fault, infilling the available accommodation space created by subsidence in the extensional pull-apart. Growth of this sedimentary profile within the half graben is thus directly related to slip on the Hosgri fault and the opening of its extensional pull apart. By measuring the heave (horizontal component of fault displacement) of the Half Graben fault relative to four identified unconformities (three Quaternary and one Pliocene-age unconformity) and relating the growth of this sediment profile to the fault geometry, independent estimates of the Hosgri fault slip rate were developed. The ages of these key unconformities were estimated based on correlation to global eustatic sea-level cycles for the Quaternary ages and as a major erosional surface throughout the study area for the Pliocene-age unconformity (PG&E, 2013). The four unconformities are identified in the 2015 PG&E PSHA (PG&E, 2015a,b) as H10 (0.020–0.007 Ma), H30 (0.135–0.125 Ma), H40 (0.625–0.245 Ma), and UNCON2 (3.5–2.7 Ma). Based on descriptions and constraints for the ages of the unconformities, this analysis was performed using a single age for each unconformity to calculate the slip rate. They are as follows: H10 = 0.020 Ma, H30 = 0.135 Ma, H40 = 0.625 Ma, and UNCON2 = 2.58 Ma. These unconformities were analyzed using seismic sections at 24 locations along the Half Graben fault. Based on the geometric constraints of the fault system and fault growth and PG&E assessments of ages for the four unconformities, the slip rate on the Hosgri fault appears to increase from a Pliocene rate of 0.21 mm/yr to a late Quaternary rate of 2.17 mm/yr. Considering the uncertainty in this analysis, the late Quaternary rate is consistent with the median rate PG&E used in its 2015 PSHA (PG&E, 2015a,b).

There are two alternative explanations for the apparent increase in rates from the Pliocene to the late Quaternary observed at this location. The increase in slip rates could simply represent an increase in activity on the Hosgri fault in the late Quaternary. Alternatively, the increase in slip rate could represent increasing cooperation and fault-linkage between the Hosgri and San Simeon faults. This latter alternative is a feature of the evolution of interacting strike-slip faults. As the faults propagate laterally so that their fault tips overlap, overall fault displacement is distributed across the intervening transfer zone, in this case, the developing half-graben. Eventually the fault tips link, at which point the fault-system-parallel slip rate on the linking Half Graben fault will equal that of the whole strike-slip fault system at this location.

## REFERENCES

PG&E. "Seismic Source Characterization for Probabilistic Seismic Hazard Analysis for the Diablo Canyon Power Plant, San Luis Obispo County, California." Report on the Results of the SSHAC Level 3 Study in Partial Compliance with NRC Letter 50.54(f), dated March 2015. 2015a

\_\_\_\_\_. "Response to NRC Request for Information Pursuant to 10 CFR 50.54(f) Regarding the Seismic Aspects of Recommendation 2.1 of the Near-Term Task Force Review from the Fukushima Dai-ichi Accident." Seismic Hazard and Screening Report, dated March 11, 2015. 2015b

\_\_\_\_\_. "Stratigraphic Framework for Assessment of Fault Activity Offshore of the Central California Coast Between Point San Simeon and Point Sal." PG&E Technical Report GEO.DCPP.TR.13.01. Pacific Gas and Electric Company. 76p. 2013.

## ACKNOWLEDGMENTS

This report was prepared to document work performed by the Center for Nuclear Waste Regulatory Analyses (CNWRA<sup>®</sup>) for the U.S. Nuclear Regulatory Commission (NRC) under Contract No. NRC–HQ–50–14–E–0001. The activities reported here were performed on behalf of the NRC Office of New Reactors. The report is an independent product of the CNWRA and does not necessarily reflect the views or regulatory position of the NRC. The authors thank Gary Walter for technical review of this report. The authors also appreciate Arturo Ramos for editorial support in the preparation of the document.

## QUALITY OF DATA, ANALYSES, AND CODE DEVELOPMENT

**DATA:** CNWRA data contained in this report meet quality assurance requirements described in the CNWRA Quality Assurance Manual. Data analyses presented in this report are documented in Scientific Notebook Number 1259. All electronic data (two dimensional seismic reflection profiles, horizon and fault interpretations, and bathymetry) were requested by and provided to the U.S. Nuclear Regulatory Commission (NRC) from Pacific Gas & Electric Company (PG&E) to support the independent evaluation of the Hosgri fault slip rate near the Diablo Canyon Power Plant. Details of the data provided by PG&E are described in the transmittal memorandum from Mr. Hans Abrahamson Ward of Lettis Consultants International to Mr. Nozar Jahangir of PG&E. A copy of this memo is documented in Scientific Notebook 1259. The source of these non-CNWRA data should be consulted for determining the level of quality assurance.

**ANALYSES AND CODES:** Maps and related Geographic Information System data were generated and plotted by the software ArcView GIS<sup>®</sup> Version 10.4, which is commercially available software that are maintained in accordance with CNWRA Technical Operating Procedure TOP–018. Fault analysis and structural modeling was performed using Move<sup>®</sup> Version 2016.1, which is also a commercially available software that is maintained in accordance with CNWRA Technical Operating Procedure TOP–018.

# 1 INTRODUCTION

## 1.1 Background

In March 2011, the U.S. Nuclear Regulatory Commission (NRC) established the Near-Term Task Force (NTTF) to conduct a systematic and methodical review of NRC processes and regulations in light of the Fukushima Dai-ichi Nuclear Power Plant accident. The NTTF was to determine whether NRC should make additional improvements to its regulatory systems considering the chain of events that led to the accident at Fukushima Dai-ichi and to make recommendations to the Commission for possible policy direction. The resulting NTTF report sets forth a series of recommendations, including Recommendation 2.1, which proposed that the NRC require licensees to re-evaluate and upgrade, as necessary, the design-basis seismic and flooding protection of systems, structures, and components important to safety for each operating reactor.

Under Recommendation 2.1, the NTTF recommended that the Commission ask licensees to re-evaluate seismic and flooding hazards against current NRC requirements and, if necessary, strengthen structures, systems, and components important to safety against the updated hazards. Specifically, NTTF Recommendation 2.1, as amended by the staff requirements memoranda associated with SECY-11-0124 and SECY-11-0137, instructs the NRC staff to issue requests for information to licensees pursuant to Sections 161.c, 103.b, and 182.a of the Atomic Energy Act of 1954, as amended, and 10 CFR 50.54(f). In accordance with the 10 CFR 50.54(f) information request, licensees of plants located in the western United States were requested to develop updated, site-specific probabilistic seismic hazard assessments (PSHAs). According to NRC recommendations, the updated PSHAs were to be consistent with Regulatory Guide (RG) 1.208, A Performance-Based Approach to Define the Site Specific Earthquake Ground Motion. In addition, the updated PSHA studies should rely on the Senior Seismic Hazard Analysis Committee (SSHAC) study, as described in NUREG/CR-6372, Recommendations for Probabilistic Seismic Hazard Analysis: Guidance on Uncertainty and Use of Experts and should be consistent with current practice, as described in NUREG-2117, Practical Implementation Guidelines for SSHAC Level 3 and 4 Hazard Studies.

The Diablo Canyon Power Plant, located on the central California coast in San Luis Obispo County, 8 km southeast of Point Buchon near Avila Beach (Figure 1-1), is owned and operated by Pacific Gas and Electric Company (PG&E) under a license from the NRC. In March 2015, PG&E submitted their response to the 10 CFR 50.54(f) information request, including their updated seismic source characterization model developed for use in the updated PSHA for the Diablo Canyon Power Plant (PG&E, 2015b). This updated seismic source characterization model (PG&E, 2015a,b) was developed following a SSHAC Level 3 process that began in June, 2011.

As part of the seismic source characterization model, a project database of all geological, geophysical, and seismological data was developed and made available to the project participants, including the Technical Integration Team. This database builds on prior PG&E databases, extending back to the initiation of the 1998 Long Term Seismic Program. Two important datasets incorporated into the project database were the series of two-dimensional (2-D) and three-dimensional (3-D) low-energy and high-energy seismic reflection datasets (PG&E, 2013) and the Cooperative Research and Development Agreement between PG&E and the United States Geological Survey (USGS). These two datasets provide the most recent information available to researchers to develop slip-rate estimates for the Hosgri fault. The NRC staff are currently evaluating the 2015 PG&E PSHA (PG&E, 2015b).

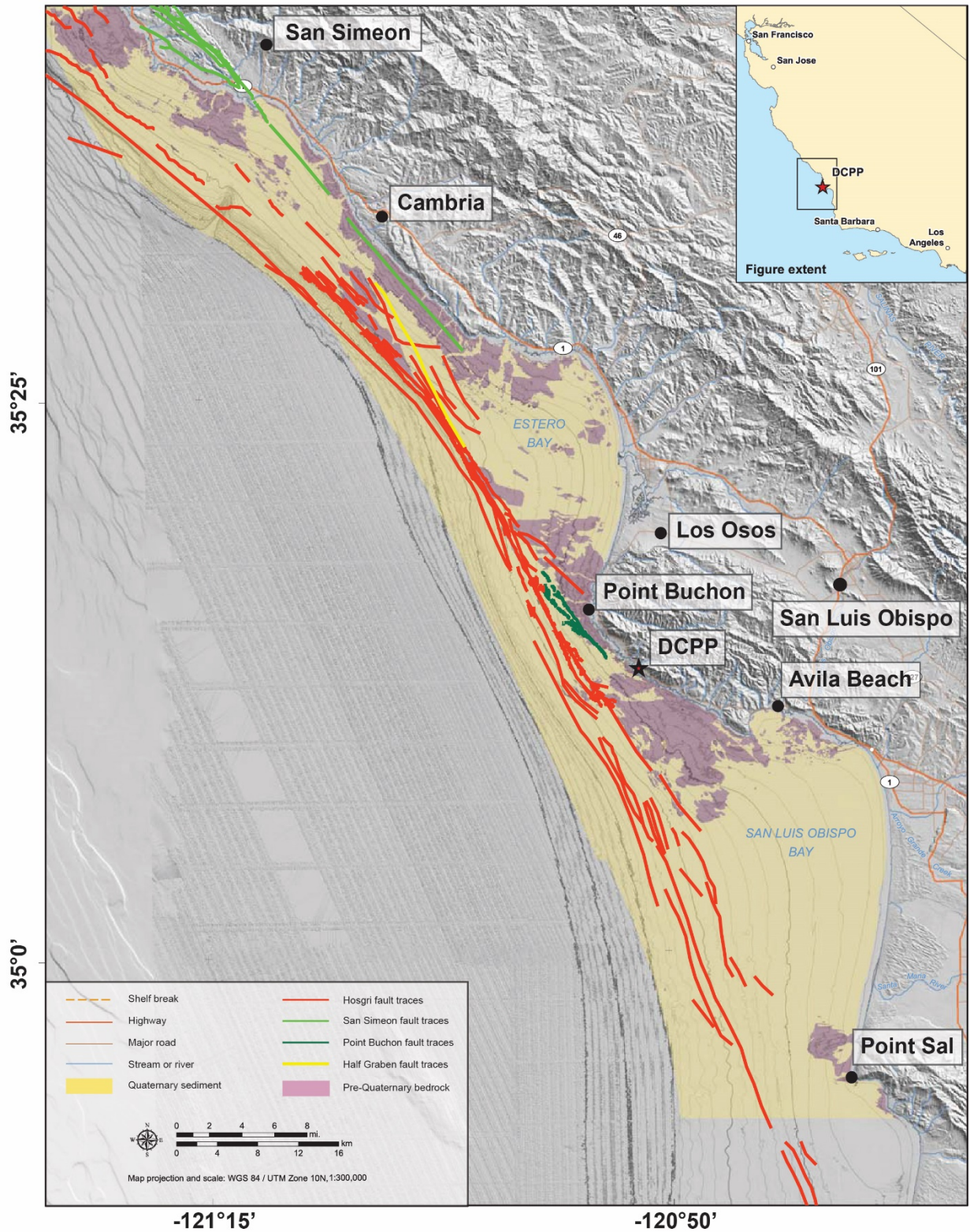


Figure 1-1. Regional Location Map [Modified From Figure 1-1 in PG&E (2014)]. Inset Shows Location in California.

## **1.2 Purpose**

The purpose of this report is to document the independent evaluation of slip rate on the Hosgri fault conducted by scientists from the Geosciences and Engineering Division (GED) of Southwest Research Institute<sup>®</sup>, under NRC Technical and Management Contract No. NRC–HQ–50–14–E–0001, Task Order NO. NRC–HQ–25–15–T–0001(49). The results of this evaluation support the NRC staff's overall technical review of the information provided by PG&E in their 2015 PSHA update (2015b). In particular, the NRC and GED staff's technical review is risk-informed because it focuses on those aspects of the PG&E report that have the strongest influence on the resulting hazard curves, either because of a direct impact on the hazard levels, large uncertainties in PSHA input values, or large uncertainties in the underlying technical bases.

In the 2015 PG&E PSHA (2015b), sensitivity studies show that up to 95 percent of the total hazard comes from the contributions of seismicity associated with the Hosgri fault. Thus, slip rate on this fault has a direct bearing on the resulting hazard levels. Given the risk-informed nature of the NRC and GED staff's review described in the preceding paragraph, a focus on assessing all the available information pertinent to the Hosgri fault slip rate directly supports the staff's overall technical review of the accuracy and adequacy of the resulting PSHA hazard curves.

## **1.3 Scope**

The scope of this report is limited to an evaluation of seismic imaging data offshore from the Diablo Canyon Power Plant in order to independently evaluate the slip rate of the Hosgri fault. This evaluation was based on 3-D geologic interpretations of 2-D offshore seismic profiles. An aggregation of offshore seismic data from Southern Estero Bay was used for interpretation and analysis using 3-D model-building, visualization, and structural restoration software. The seismic reflection data for this analysis were provided by PG&E (as described previously), including the USGS 2008-2009 high-resolution sparker tracklines (PBS) and the 1986 joint PG&E and Alaska COMAP lines (COMAP). Ages for the unconformities used in the analyses of the seismic stratigraphy were taken directly from the stratigraphic framework detailed in PG&E's 2013 technical report to the Central California Public Utilities Commission (PG&E, 2013).

## 2 ANALYSIS

### 2.1 Seismotectonic Setting

The Diablo Canyon Power Plant is located along the central California coast in the Irish Hills within the northwestern-most portion of the San Luis Range. The San Luis Range is one of many northwest to north-northwest trending ranges that make up the central Coast Ranges of California. Most of the Central California Coast Ranges consist of uplifted blocks that formed in response to distributed dextral transpression arising from the relative motions between the North American and Pacific plates (Lettis and Hanson, 1992; Lettis et al., 1994, 2004; McLaren and Savage, 2001). Most of the horizontal motion between the North American and Pacific plates is accommodated by slip on the San Andreas Fault, which lies approximately 70 km to the northeast of the Diablo Canyon Power Plant. The remaining component of horizontal motion along this plate boundary is accommodated by slip on a series of coast-parallel strike-slip faults, including the Hosgri fault.

The Hosgri fault is located just a few kilometers offshore south-central California and forms the eastern boundary of the offshore Santa Maria Basin (PG&E, 1988; Clark et al., 1991; Steritz and Luyendyk, 1994). Within the regional tectonic setting, the Hosgri fault forms the southernmost segment of the 410 km-long San Gregorio-San Simeon-Hosgri fault system. This fault system is one of several coast-parallel strike-slip fault zones that accommodate relative plate motions between the Pacific and North American tectonic plates that is not directly attributed to the San Andreas Fault (Atwater, 1989; Argus and Gordon, 2001; Lettis et al., 2004).

Characterization of the fault is primarily derived from traditional marine seismic reflection data and single-channel, high-resolution sparker data. It has been mapped along its entire length using petroleum industry multichannel seismic-reflection data that images the traces of the fault to 3 km depth beneath the seafloor (PG&E, 1988, 1991; and Willingham et al., 2013). Significant sections of the Hosgri fault were also remapped using single-channel, high-resolution U.S. Geological Survey (USGS) sparker data (Johnson and Watt, 2012; PG&E, 2014). Based on these data, the Hosgri fault is interpreted by Pacific Gas and Electric Company (PG&E) and USGS, among others, as a 160 km long, right-lateral, strike-slip fault that extends from its intersection with the San Simeon fault north of Point Estero to the south-southeast, where it tips at Purisima Point (e.g., Hoskins and Griffiths, 1971; Gawthrop, 1978; Hanson et al., 2004).

In the immediate vicinity of the Diablo Canyon Power Plant, the Hosgri fault trends N 25° to N 30° W and comprises multiple fault traces, with individual segment lengths up to 18 km long that overlap *en echelon*, forming a fault zone up to 2.5 km wide (Figure 1-1). In the seismic-reflection profiles, fault traces appear to be vertical to steeply dipping in the uppermost sedimentary section, but some of the fault traces below about 1 km depth appear to be subvertical or dipping steeply to the east.

Earthquake focal mechanisms in south central California are mainly reverse and strike-slip, consistent with the right-lateral transpressional tectonic setting of the region (e.g., McLaren and Savage, 2001; Hardebeck, 2010). Focal mechanisms and the spatial distribution of seismic events along the Hosgri fault in the subsurface are predominantly right-lateral strike-slip on a nearly vertical to steeply east-dipping fault zone, with active seismicity to a depth of about 12 km (McLaren and Savage, 2001; Hardebeck, 2010; McLaren et al., 2008). There is also abundant seismicity recorded beneath the Diablo Canyon Power Plant and to the east of the Hosgri fault, but the rates of seismicity diminish considerably west of the Hosgri fault within the Santa Maria basin.

Numerous researchers have investigated the slip rate of the Hosgri fault since it was first identified in the late 1970's. Estimates of the slip rate on the Hosgri fault in the vicinity of the Diablo Canyon Power Plant from published papers and reports range from 1 to 8 mm/yr, but estimates based on local geologic features show slip rates less than about 5 mm/yr (Table 2-1). In the 2015 PSHA (PG&E 2015a,b), PG&E analyzed or re-analyzed evidence of fault slip at four sites along the Hosgri fault. These analyses included analysis or re-analysis of (i) an offset marine terrace strandline near San Simeon (referred to as Oso Terrace), (ii) offset of the shoreface of a late Pleistocene sand spit between Morro Bay and Point San Simeon (referred to as the Cross-Hosgri slope), (iii) dextral separation of a buried paleo-channel in Estero Bay, and (iv) dextral separation of a buried paleo-channel near Point Sal. Median slip rates based on amount of offset and ages of these four offset markers ranged between 0.8 mm/yr (Point Sal) and 2.5 mm/yr (Cross-Hosgri slope), with a weighted mean from all four sites of 1.7 mm/yr  $\pm$  0.7 mm/yr (1 standard deviation).

## **2.2 Transtensional Features Along the Hosgri Fault**

Detailed analysis of three-dimensional (3-D) seismic reflection data along the Hosgri fault shows considerable segmentation and structural complexity including closely associated transpressional and transtensional deformation along the Hosgri fault southeast of the Diablo Canyon Power Plant (Kluesner and Brothers, 2016). Transtensional segments of the Hosgri fault zone offshore from Cambria—northwest of the Diablo Canyon Power Plant—have been identified using analysis of high-energy multichannel seismic-reflection data (PG&E, 1988, 1991; Willingham et al., 2013). One of these features is an extensional half graben bounded by a 15 km long extensional fault, named the Half Graben fault (Figure 2-1). This fault lies entirely between the traces of the Hosgri and San Simeon faults, and has been interpreted as part of a pull-apart basin developed within a right-step between two right-lateral strike-slip faults, the Hosgri Fault Zone to the south and the San Simeon fault to the north (DiSilvestro et al., 1990; Lettis et al., 1990; Hanson et al., 2004). This extensional basin is asymmetric, shallows to the northeast, and contains southwest-dipping reflectors (Figures 2-2, 2-3, and 2-4) that define layers that thicken toward the southwest and record progressive sedimentation into a developing half-graben forming in the hanging wall of a northeast dipping fault. Evidence from earthquake hypocenters and seafloor scarps suggests that the Half Graben Fault system is an active, northeast-dipping extensional fault (PG&E, 2014). In addition, two other extensional grabens (Graben A and Graben B; PG&E, 2014) have been recognized offshore south of the Half Graben fault, east of the Hosgri Fault Zone, and approximately 10 km northwest of the Diablo Canyon Power Plant.

Because the Half Graben fault is not parallel to the regional slip direction on the Hosgri fault system, and exists in a right step in a right-lateral strike-slip system, this fault accommodates a component of extension generated by horizontal slip on the Hosgri fault system. There is no direct evidence (e.g., piercing points) to determine whether displacement on the Half Graben fault is dip-slip or oblique-slip. However, the fault-perpendicular horizontal component of the displacement (heave) projected onto the strike of the Hosgri fault provides a measure of the Hosgri fault-parallel slip. As the pull-apart basin developed, sediments accumulated along the fault, infilling the available accommodation space created by seafloor subsidence in the extensional pull-apart (Figures 2-2 and 2-3). By measuring the heave (horizontal component of fault displacement) of the Half Graben fault relative to four identified unconformities and relating the growth of this sediment profile to the fault geometry, we developed independent estimates of the Hosgri fault slip rate.

The ages of the four key unconformities were estimated based on correlation to global eustatic sea-level cycles for the Quaternary-ages and as a major erosional surface throughout the study area for the Pliocene-age unconformity (PG&E, 2013). These four unconformities are Pleistocene age H10 (0.020-0.007 Ma), H30 (0.135-0.125 Ma), H40 (0.625–0.245 Ma), and a basal Pliocene unconformity UNCON2 (3.5-2.58 Ma). Discussion of the range of possible ages for each unconformity and the constraints of these ages are provided in PG& E (2013; Section 6.1-6.7, pp. 27–34). Based on descriptions and constraints for the ages of the unconformities in PG&E (2013), we performed this analysis using a single age for each unconformity to calculate the slip rate. They are as follows, H10 = 0.020 Ma, H30 = 0.135 Ma, H40 = 0.625 Ma, and UNCON2 = 2.58 Ma.

**Table 2-1. Hosgri Fault Slip Rates From Published Sources\***

<b>Fault segment</b>	<b>Low horizontal rate, mm/yr</b>	<b>High horizontal rate, mm/yr</b>	<b>Slip rate single value, mm/yr</b>	<b>Low vertical rate, mm/yr</b>	<b>High vertical rate, mm/yr</b>	<b>Highest slip-vector-parallel rate, mm/yr</b>	<b>Data type</b>	<b>Source</b>
Whole fault	1.00	3.00					Map restoration	Sorien et al. (1999)
Whole fault	3.45	7.14					Paleomagnetic data	Hornafius et al. (1986)
San Simeon-Hosgri stepover to Los Osos	1.00	3.00		0.03	0.30	3.01	Marine terrace, fluvial deposits mapping; reflection seismic analysis of unconformities	Hanson and Lettis (1994)
Los Osos to SW Boundary faults	0.80	2.80		0.08	1.40	3.13	Marine terrace, fluvial deposits mapping; reflection seismic analysis of unconformities	Hanson and Lettis (1994)
SW Boundary faults to Casmalia FZ	0.70	2.70		0.05	1.40	3.04	Marine terrace, fluvial deposits mapping; reflection seismic analysis of unconformities	Hanson and Lettis (1994)
Casmalia FZ to Lion's Head FZ	0.60	2.60		0.03	2.60	3.68	Marine terrace, fluvial deposits mapping; reflection seismic analysis of unconformities	Hanson and Lettis (1994)
Lion's Head FZ to Southern termination	0.55	2.55		0.08	2.55	3.61	Marine terrace, fluvial deposits mapping; reflection seismic analysis of unconformities	Hanson and Lettis (1994)

**Table 2-1. Hosgri Fault Slip Rates From Published Sources (Continued)**

<b>Fault segment</b>	<b>Low horizontal rate, mm/yr</b>	<b>High horizontal rate, mm/yr</b>	<b>Slip rate single value, mm/yr</b>	<b>Low vertical rate, mm/yr</b>	<b>High vertical rate, mm/yr</b>	<b>Highest slip-vector-parallel rate, mm/yr</b>	<b>Data type</b>	<b>Source</b>
San Gregorio-Hosgri			3.00				Regional geodetic analysis	Argus & Gordon (2001)
Hosgri, whole fault			8.04				Regional stratigraphic correlations	Burnham (2009)
Hosgri, whole fault	-1.80	-0.40					Computer model of gps velocities	Zeng & Shen (2014)
San Gregorio	3.80	3.90					Computer model of gps velocities	Zeng & Shen (2014)
Hosgri, whole fault	1.00	3.00					Offset of Pleistocene shoreface	Johnson et al. (2014)
Hosgri, Point Sal	0.40	5.10	1.85				Offset of Pleistocene channels	PG&E (2015a)
Hosgri, channels A and B	0.20	4.50	1.80				Offset of Pleistocene channels	PG&E (2015a)
Hosgri, Estero Bay	0.20	3.60	1.40				Offset of Pleistocene channels	PG&E (2015a)

\* Negative values indicate left-lateral slip, Positive values indicate right-lateral slip

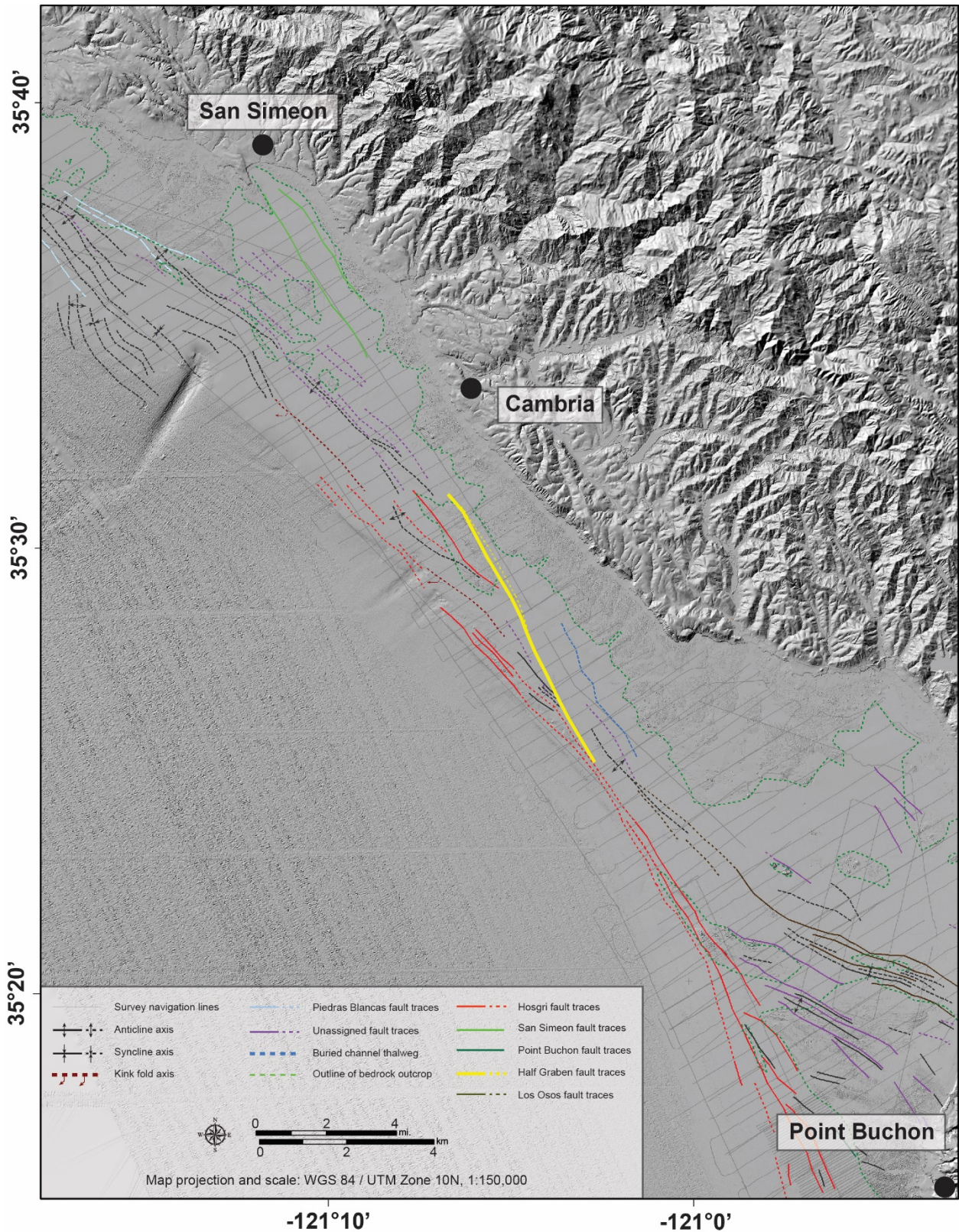


**Figure 2-1. Location Map [Modified From Figure 1.2-1 in PG&E (2014)]. Map Shows Full Trace of the Half Graben Fault With Respect to the Hosgri Fault Trace**

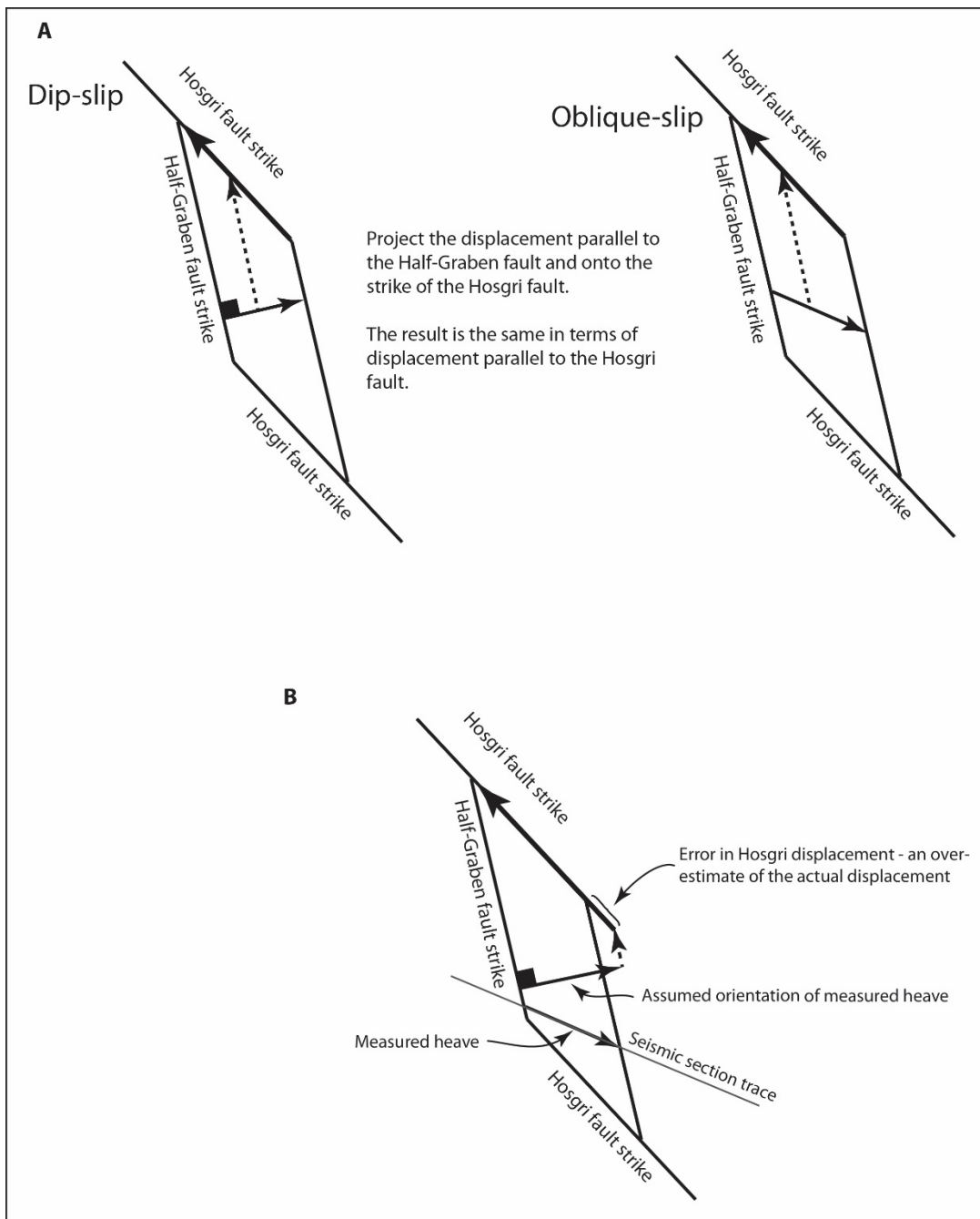


**Figure 2-2. (A) Map View of the Principal Geometric Elements of the Hosgri and Half Graben Faults, and Illustrating How the Magnitude of Hosgri-Parallel Slip Is Independent of the Direction of Slip on the Half Graben Fault. (B) Map View Similar to (A) Showing the Nature and Magnitude of Error Introduced by Assuming That the Seismic Section Trace in Which the Half Graben Heave Is Measured Is Perpendicular to the Half Graben Fault Trace.**

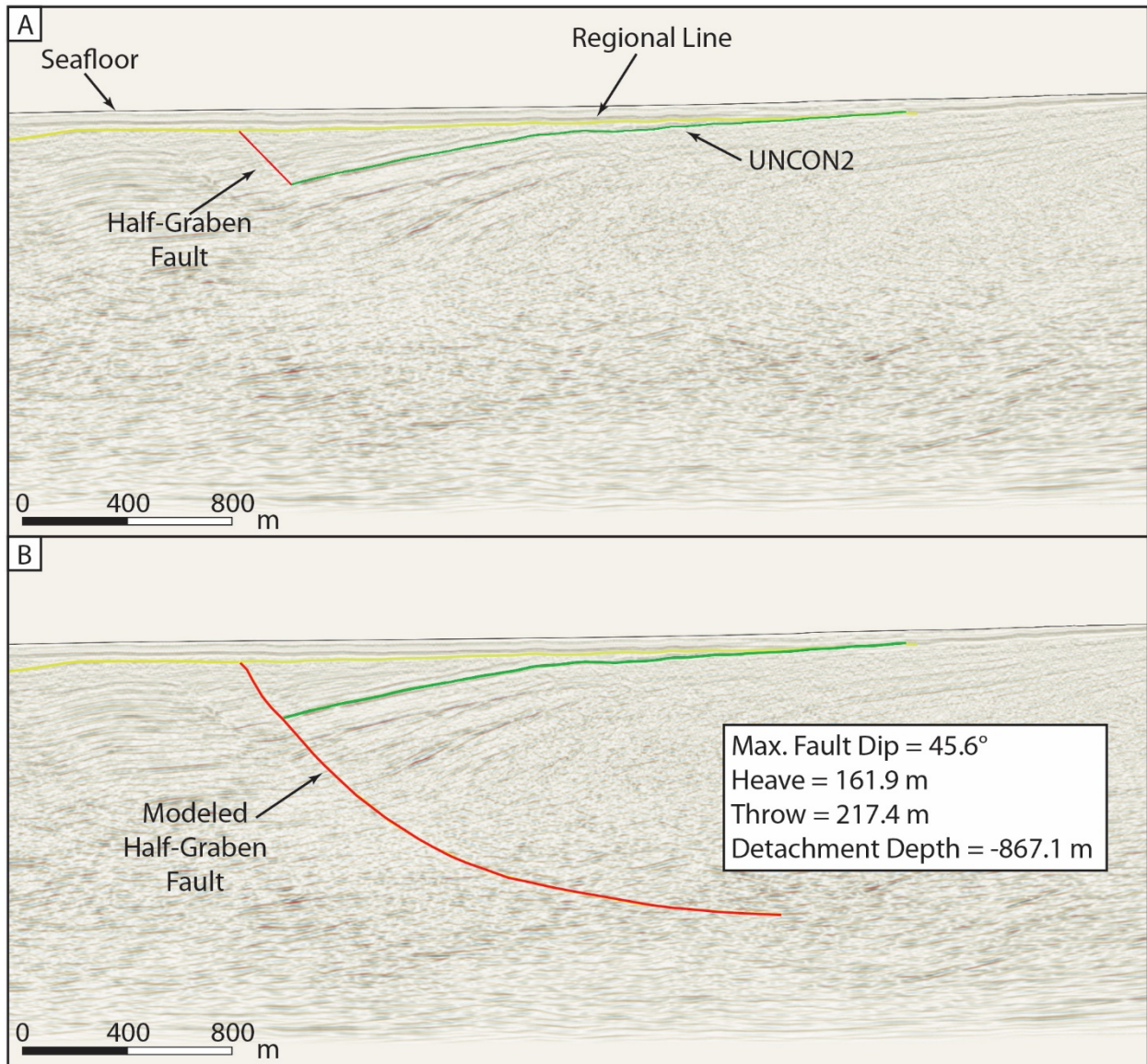


**Figure 2-3. COMAP Seismic Reflection Example. (A) Shows the Initial Unconformity Horizon and Fault Interpretations and (B) Shows the Modeled Half Graben Geometry and Fault Attributes.**

## 2.3 Methodology

### *Seismic sections and depth conversion*

An aggregation of offshore seismic data from Southern Estero Bay was used for interpretation and analysis using 3-D model-building, visualization, and structural restoration software. All seismic reflection data for this analysis was provided by PG&E in two-way travel time (TWT)

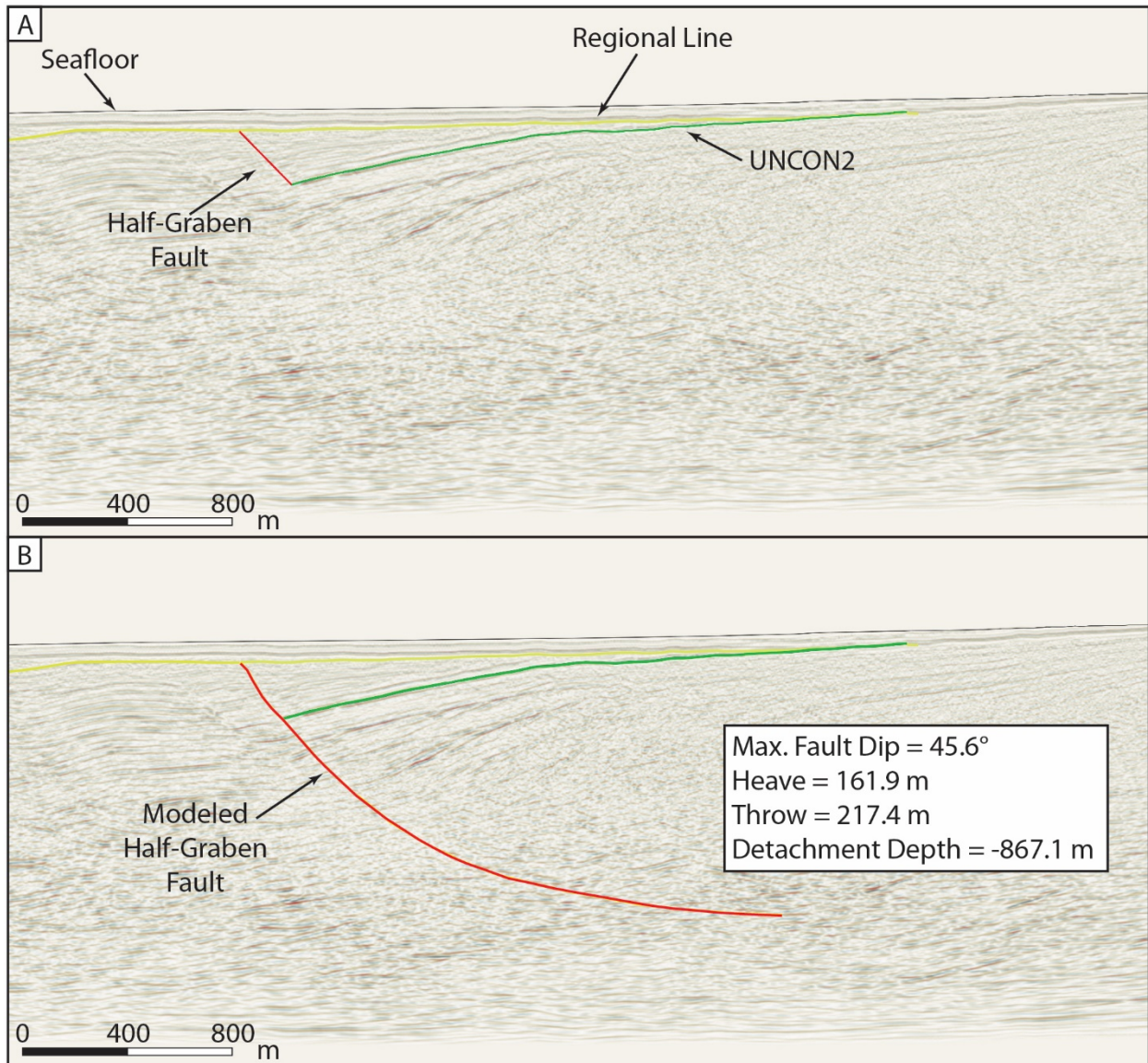


**Figure 2-4. High-Resolution Sparker Tracklines (PBS) Seismic Reflection Example. (A) Shows the Initial Unconformity Horizon and Fault Interpretations and (B) Shows the Modeled Half Graben Geometry and Fault Attributes.**

including the USGS 2008-2009 high-resolution sparker tracklines (PBS) and the 1986 joint PG&E and Alaska COMAP lines (COMAP) two-dimensional (2-D) seismic reflection, horizon interpretations, and fault interpretations. The only seismic data provided that was depth converted were the sediment thickness contour and seafloor bathymetry for a subset of the COMAP and PBS data domain.

All other data were depth-converted using two separate velocity models that were created using a constant velocity of 1,600 m/s for the sub-seafloor sediment. Two models were required because the PBS data and the COMAP data each had a different seismic reference datum. The depth conversion workflow was as follows:

1. Load horizon interpretation files as point data.
2. Convert horizon point data to horizon line interpretations.
3. Interpret the seafloor in TWT on each COMAP and PBS 2-D seismic line that was provided.
4. Create surfaces from each horizon line interpretation (25 × 25 m cell size).
5. Create two new velocity models using a constant velocity of 1,600 m/s. (The bathymetric data provided by PG&E were used as the depth datum for each model.)
6. Match the TWT-interpreted seafloor for the COMAP and PBS to the bathymetric data provided by PG&E.
7. Convert the original unconformity horizons interpretations, fault interpretations, and 2-D seismic reflection data from TWT time to depth once the velocity models were created

All data (2-D seismic, horizons, and faults) in this analysis have been depth-converted and all analyses were performed using equal vertical and horizontal scales (i.e., no vertical exaggeration).

### ***Displacement analysis***

There are three components to the geometric analysis used here. The first is an interpretation from seismic reflection profiles (PG&E, 2014) of the vertical displacement (throw) of submarine Pleistocene and Pliocene unconformities (PG&E, 2013, 2014) by the Half Graben fault, and the shallow portion of the fault geometry. The second component is the application of the vertical simple shear or “Chevron” method (Verrall, 1981; Gibbs, 1983; 1984) and the inclined shear method (White et al., 1986; Rowan and Kligfield, 1989) to generate fault geometries at depth. Third, the horizontal component (heave) of the Half Graben fault displacement is corrected to determine the slip in the direction of the Hosgri fault, and this slip magnitude is divided by the age of the unconformity to provide a slip rate estimate.

Initial interpretations of the Pleistocene unconformities and the seafloor locations of the Half Graben fault were provided by PG&E. The unconformity and fault interpretation were honored to the extent practicable; however, in many cases the interpretations were adjusted to improve the match with the seismic reflectors. Figure 2-3 illustrates an example of a COMAP seismic line (Line 47), UNCON2 unconformity (2.58 Ma), and the shallow portion of the Half Graben fault. Applying the vertical and inclined shear methods for fault construction generates a range of fault geometries (Figure 2-3 b and Figure 2-4 b). The vertical and inclined shear methods assume plane strain with no movement of material in or out of the 2-D plane. The fault geometry is modeled using the geometry of a deformed hanging wall horizon and an inferred regional level to predict the location and shape of a fault at depth that terminate at a detachment depth (Verrall, 1981; White et al., 1986; Dula, 1991). This method is based on area balance and assumes that the hanging wall fold geometry is controlled by the underlying fault geometry and the assumption that the footwall remains rigid. Finally, the horizontal component (heave) of this displacement was projected onto the displacement direction of the main Hosgri fault to give the Hosgri-parallel displacement amount, and this was divided by the age of the unconformity to yield a slip rate.

The Half Graben fault interpretations provided by PG&E were primarily used to delineate the Half Graben basin, and were not intended for detailed analysis. The faults in this analysis were modeled using a constant heave method to construct fault geometries at depth (Verrall, 1981; White et al., 1986; Rowan and Kligfield, 1989). The goal was to model the “best case” fault geometry for each seismic line. For the purpose of this analysis, “best case” means the fault geometry that provided the closest match to the seismic reflectors along the full extent of the fault trace to depth. To provide a range of geometries for a given initial fault interpretation, a range of shear angles was used so that the geometry of the fault could be adjusted without having to deviate too far from the initial near-surface interpretation. Because the goal of the analysis was to match the seismic data using a single Half Graben fault, the “best case” shear angle used to model the Half Graben fault geometry varies from line to line. The analysis described above was applied to 24 seismic reflection profiles that are approximately perpendicular to the strike of the Half Graben fault. This includes 7 COMAP and 17 PBS lines.

The Half Graben fault extends almost to the San Simeon fault, the southern termination of which is also a series of splays similar to the Hosgri fault. It is not clear that displacement is fully transferred from the Hosgri fault to the San Simeon fault—thus the Half Graben basin may be an extensional basin within the transfer zone and not a full pull-apart basin. The location of the Half Graben fault is near the tips of two faults where displacement approaches zero. In such locations, displacement is transferred from one fault to the other via a relay structure or accommodation zone by a combination of rotation and distributed deformation.

Faults in this situation can be described as soft linked (e.g., Rosendahl et al., 1986; Rowland and Sibson, 2001). Once a through-going fault connection is developed (Rahe et al., 1998), the faults are described as hard linked. Once faults are hard linked, the linkage zone is no longer at the tip of a fault or fault segment but instead along the extent of the fault where the through-going fault will carry most of the displacement. Consequently, the rate of fault displacement in the zone of linkage can accelerate over time as soft linkage evolves to hard linkage.

Whether displacement on the Hosgri and Simeon fault systems is hard or soft linked, horizontal displacement accommodated by the Half Graben fault represents only a portion of the displacement on the Hosgri-San Simeon fault system. The slip rate calculated for the Hosgri-San Simeon system from analysis of the Half Graben basin and fault structure will therefore be a minimum estimate, although because it is the largest extensional system in the transfer zone it probably represents the majority of slip.

## **2.4 Dip-Slip Versus Oblique-Slip on the Half Graben Fault**

Because the Half Graben fault is not parallel to the regional slip direction on the Hosgri fault system, and because it exists in a right step in a right-lateral strike-slip system, it accommodates a component of extension generated by the regional strike-slip system. This is attested to by the sedimentary growth wedges that thicken towards the Half Graben fault within the Half Graben basin (Figures 2-3 and 2-4).

The fault-perpendicular horizontal component of the displacement was measured and then projected onto the strike of the Hosgri fault to determine the horizontal component of the Hosgri fault-parallel slip (Figure 2-2). Projection of the strike-perpendicular heave onto the Hosgri fault parallel to the strike of the Half Graben fault will yield the Hosgri-fault-parallel displacement regardless of the slip direction on the Half Graben fault. Error may be introduced, however, if the seismic sections used for the analysis are not perfectly perpendicular to the Half Graben

fault, but are assumed to be so. This will overestimate the slip by an amount related to the angle of deviation from perpendicularity to the Half Graben fault strike. The seismic sections used for this analysis are not perfectly perpendicular to the Half Graben fault (Figure 2-2), with angular deviations of 70° to 107°, but averaging 87.6° (Table 2-2).

The analysis presented here focuses on the Half Graben fault zone, however, it may be possible to perform similar analyses on the other extensional grabens in the region. Interpretation of three Pleistocene age unconformities and one Pliocene age unconformity into the Half Graben basin allows fault heave to be measured for each unconformity time interval (H10 = 0.020 Ma, H30 = 0.135 Ma, H40 East = 0.625 Ma, UNCON2 = 2.58 Ma).

## 2.5 Uncertainty in Slip Rate

There are a number of uncertainties in this estimate of the Hosgri Fault slip rate, some of these can be reduced by further work, and some are inherent in the nature of the data. The following subsections summarize sources of uncertainty for slip rate estimates.

### *Ages of unconformities*

Description and constraints of the ages for each unconformity in this analysis can be found in PG&E (2013; Section 6.1-6.7, pp. 27–34). For this analysis, a single age for each unconformity was used. For the Quaternary ages [specifically H10 and H40; (PG&E, 2013, Section 6.6, pp. 32–33)], the younger age ranges had inconsistencies between the age models and the observations of the interpreted horizons across the study area. Therefore, to be consistent, the older age range for each of the Quaternary unconformities was used in this analysis. Contrary to the Quaternary unconformities, the top of Pliocene age unconformity is well observed throughout the study area and is represented by a high-amplitude basal reflector underlying the subhorizontal Quaternary sediments (PG&E, 2013). The age range is constrained by microfossil data from wells (Willingham et al., 2013), and for this analysis the younger end of the age range was used. Below is the age description for each unconformity in the study.

- H10 is the youngest unconformity in this analysis and is considered to represent the late Quaternary transgressive sequence. The age range for this unconformity is 0.20 to 0.007 Ma (PG&E, 2013). The age for this unconformity used in this analysis is 0.20 Ma.
- H30 represents a late Quaternary transgressive surface and is the most widely correlated unconformity in the study area. The age range for this unconformity is 0.135 to 0.125 Ma. The age for this unconformity used in this analysis is 0.135 Ma.
- H40 East is the deepest regionally correlated late Quaternary unconformity. It is also the most difficult to correlate and therefore the lowest confidence of all the unconformity surfaces. The age range for this unconformity is 0.625 to 0.245 Ma. The age for this unconformity used in this analysis is 0.625 Ma.
- UNCON2 is the oldest and deepest unconformity (referred to as ELP in PG&E, 2014). It represents the top of the Neogene unconformity in the Half Graben Basin. The age range for this unconformity is 3.5 to 2.58 Ma. The age for this unconformity used in this analysis is 2.58 Ma.

Age estimates for H10 and H40 vary by factors of 2.86 and 2.55 respectively, which would lead to a commensurate range of potential slip rate estimates if the ranges of unconformity ages

<b>Table 2-2. Possible Error in the Half Graben Fault Analysis Arising From Nonideal Cross-Section Orientation (Uncon 2)</b>						
<b>Line</b>	<b>Angle with Half-Grabens fault trace, degrees</b>	<b>Measured heave displacement, m</b>	<b>Calculated displacement assuming sections are perpendicular to Half-Grabens trace</b>	<b>Modeled displacement, m</b>	<b>Error</b>	<b>% Error</b>
COMAP 51	85	66.50	256.94	255.96	0.98	0.38
COMAP 49	70	30.50	117.84	110.74	7.11	6.42
COMAP 47	75	161.90	625.53	604.22	21.31	3.53
COMAP 45	99	306.70	1185.00	1170.41	14.59	1.25
COMAP 43	76	159.20	615.10	596.83	18.27	3.06
COMAP 41	84	49.50	191.25	190.21	1.05	0.55
COMAP 39	84	33.60	129.82	129.11	0.71	0.55
PBS 210	98	305.30	1179.59	1168.11	11.48	0.98
PBS 209	98	331.00	1278.89	1266.44	12.45	0.98
PBS 206	107	448.30	1732.10	1656.41	75.68	4.57
<b>Average angle</b>	<b>87.6</b>					
<b>Half-Grabens trace to Hosgri trace = 15 degrees</b>						

were considered. Reducing uncertainty in these ages could significantly reduce uncertainty in the slip rate estimates.

### ***Fault dip***

Fault dip is interpreted using the seismic reflection data with the initial location of the Half Graben fault trace provided by PG&E. In most cases, the provided fault interpretations do not quite honor the visible offsets of seismic reflectors; therefore, for this analysis the surface location of the fault is used and then the interpretation at depth that best honors the fault-truncated seismic reflectors is used to determine the fault dip. Fault dip strongly influences the heave (horizontal) component of displacement, which is a key parameter used in calculating the slip rate.

### ***Quality of seismic reflection data***

For this analysis, two different seismic reflection data sets (PBS and COMAP) were used and yielded similar results. Both data sets consist of 2-D profiles collected under different conditions with different parameters. Resolution limits of data influence the detail of fault, horizon, and displacement measurements.

### ***Accuracy of picks for unconformity horizons***

Accurate picking of unconformity horizons is essential because displacement measurements are directly controlled by the fault gaps in these interpreted unconformities. Inaccuracies in precise interpretation of the unconformity positions on the footwall and hanging wall are a source of uncertainty.

### ***Displacement on other smaller-displacement faults***

In most of the seismic reflection profile sections, the Half Graben fault appears as one major fault, but other smaller-displacement faults are present in the sections. These additional smaller displacement faults were not analyzed in detail in this study and their inclusion in the analysis would increase the overall displacement and related slip rate estimates. Based on the small displacements on these faults, it is estimated that the influence on displacement and slip rate would be <10 percent.

### ***Apparent offset on the Half Graben fault***

As discussed in section 2.4, if displacement on the Half Graben fault is not pure dip-slip, the methodology used here will faithfully characterize the Hosgri Fault-parallel component of slip. Therefore, exact slip direction on the Half Graben fault is not considered a significant source of uncertainty. Error introduced by assuming that the seismic sections are perpendicular to the fault trace and is in the profile direction has been quantified (Table 2-2) and will always generate a higher estimate of slip rate.

### 3 RESULTS

The final fault geometries from unconformity horizon interpretations and initial Half Graben fault geometries were constructed for 24 two-dimensional (2-D) seismic reflection profiles. For the 24 profiles, a total of 59 fault models were generated, one for each unconformity horizon interpretation that was provided by Pacific Gas and Electric Company (PG&E) in each of the cross sections. For each fault that was modeled, fault dip, displacement, heave, throw, and slip rate parallel to the Hosgri fault were determined (Table 3-1). Near-surface fault dip was interpreted on each cross section, along with the unconformity(ies) in the hanging wall of the fault. For this analysis, the footwall position of the unconformities are assumed to be at the first major reflector beneath the seafloor. The first major reflector was chosen because it matches reflectors on the east side of the Half Graben Basin where the unconformities initiate. Lining up these reflectors forms the regional line shown on Figures 2-3 and 2-4. For all Half Graben fault geometries, the fault dip range is between 27° and 63.8° with an average of 46.3°. The displacements range from 3.4 to 606.8 m with an average of 113.4. The heaves range from 1.7 to 449.5 m with an average of 80.1 m. The throws range from 2.9 to 354.6 m with an average of 76.9 m. The slip rates parallel to the Hosgri fault range from 0.02 to 1.81 mm/yr with an average of 0.314 mm/yr. Figure (3-1 a-e) shows the slip rate for each unconformity. The average slip rates based on displacements of each unconformity are as follows: (i) UNCON2 = 0.21 mm/yr, (ii) H40 East = 0.44 mm/yr, (iii) H30 = 0.98 mm/yr, and (iv) H10 = 2.17 mm/year (see Figures 3-2, 3-3, and 3-4).

**Table 3-1. Results From Fault Analysis**

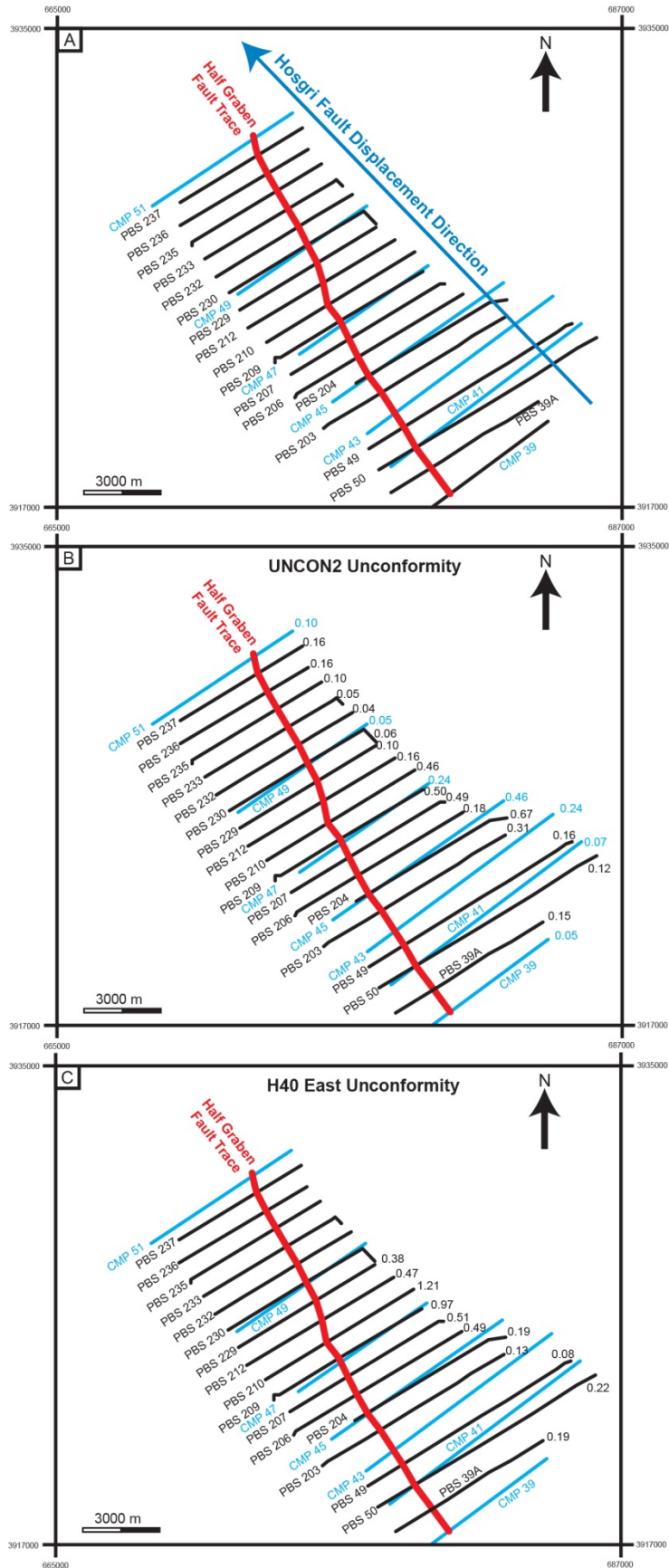
Seismic Line	Unconformity	Age of Unconformity	Half Graben Fault Dip	Displacement (m)	Heave (m)	Throw (m)	Slip Rate Parallel to the Hosgri Fault (mm/year)
PBS 49	H10	0.020	60.0	3.40	1.70	2.90	0.33
PBS 235	H10	0.020	34.0	20.14	16.70	11.30	3.23
PBS 233	H10	0.020	60.0	6.00	3.00	4.80	0.58
PBS 232	H10	0.020	60.8	7.17	3.50	6.00	0.68
PBS 230	H10	0.020	53.9	19.52	11.50	15.80	2.22
PBS 229	H10	0.020	55.9	21.23	11.90	17.70	2.30
PBS 212	H10	0.020	52.6	14.16	8.60	11.35	1.66
PBS 210	H10	0.020	37.0	29.43	23.50	17.65	4.54
PBS 209	H10	0.020	29.8	21.32	18.50	10.50	3.57
PBS 207	H10	0.020	38.0	16.37	12.90	10.15	2.49
PBS 204	H10	0.020	42.2	16.20	12.00	10.90	2.32
PBS 50	H30	0.135	55.0	36.26	20.80	29.50	0.60
PBS 49	H30	0.135	60.0	13.20	6.60	11.50	0.19
PBS 39A	H30	0.135	40.0	13.58	10.40	8.70	0.30
PBS 232	H30	0.135	60.2	34.81	17.30	29.80	0.50
PBS 230	H30	0.135	53.4	59.88	35.70	49.20	1.02
PBS 229	H30	0.135	55.9	59.40	33.30	49.30	0.95
PBS 212	H30	0.135	53.4	60.88	36.30	47.50	1.04
PBS 210	H30	0.135	28.9	134.21	117.50	65.30	3.36
PBS 209	H30	0.135	28.3	76.89	67.70	33.40	1.94
PBS 207	H30	0.135	39.4	47.75	36.90	28.90	1.06
PBS 206	H30	0.135	39.2	35.49	27.50	16.00	0.79
PBS 204	H30	0.135	42.2	33.61	24.90	22.80	0.71
PBS 203	H30	0.135	48.1	14.82	9.90	11.10	0.28
PBS 50	H40 East	0.625	55.0	61.02	35.00	49.70	0.22
PBS 49	H40 East	0.625	60.0	25.20	12.60	21.90	0.08

**Table 3-1. Results From Fault Analysis**

<b>Seismic Line</b>	<b>Unconformity</b>	<b>Age of Unconformity</b>	<b>Half Graben Fault Dip</b>	<b>Displacement (m)</b>	<b>Heave (m)</b>	<b>Throw (m)</b>	<b>Slip Rate Parallel to the Hosgri Fault (mm/year)</b>
PBS 39A	H40 East	0.625	40.0	41.12	31.50	26.40	0.19
PBS 229	H40 East	0.625	52.3	101.55	62.10	91.70	0.38
PBS 212	H40 East	0.625	52.3	124.44	76.10	99.50	0.47
PBS 210	H40 East	0.625	30.4	227.01	195.80	118.20	1.21
PBS 209	H40 East	0.625	33.0	187.08	156.90	85.90	0.97
PBS 207	H40 East	0.625	33.0	98.37	82.50	64.75	0.51
PBS 206	H40 East	0.625	39.2	101.43	78.60	42.20	0.49
PBS 204	H40 East	0.625	42.2	42.39	31.40	28.80	0.19
PBS 203	H40 East	0.625	48.1	31.74	21.20	25.60	0.13
COMAP 51	UNCON 2	2.580	32.9	79.20	66.50	43.00	0.10
COMAP 49	UNCON 2	2.580	63.8	69.08	30.50	62.10	0.05
COMAP 47	UNCON 2	2.580	45.6	231.40	161.90	217.40	0.24
COMAP 45	UNCON 2	2.580	50.0	477.14	306.70	256.80	0.46
COMAP 43	UNCON 2	2.580	58.4	303.82	159.20	225.60	0.24
COMAP 41	UNCON 2	2.580	46.6	72.04	49.50	52.30	0.07
COMAP 39	UNCON 2	2.580	50.8	53.16	33.60	40.90	0.05
PBS 50	UNCON 2	2.580	55.0	134.77	77.30	109.90	0.12
PBS 49	UNCON 2	2.580	60.0	214.00	107.00	185.10	0.16
PBS 39A	UNCON 2	2.580	40.0	128.19	98.20	82.00	0.15
PBS 237	UNCON 2	2.580	27.0	117.28	104.50	54.00	0.16
PBS 236	UNCON 2	2.580	33.0	125.68	105.40	56.80	0.16
PBS 235	UNCON 2	2.580	34.0	80.33	66.60	45.40	0.10
PBS 233	UNCON 2	2.580	60.0	65.20	32.60	52.00	0.05
PBS 232	UNCON 2	2.580	55.9	44.41	24.90	43.10	0.04
PBS 230	UNCON 2	2.580	55.9	71.53	40.10	55.30	0.06
PBS 229	UNCON 2	2.580	55.9	117.54	65.90	97.50	0.10

**Table 3-1. Results From Fault Analysis**

<b>Seismic Line</b>	<b>Unconformity</b>	<b>Age of Unconformity</b>	<b>Half Graben Fault Dip</b>	<b>Displacement (m)</b>	<b>Heave (m)</b>	<b>Throw (m)</b>	<b>Slip Rate Parallel to the Hosgri Fault (mm/year)</b>
PBS 212	UNCON 2	2.580	54.7	180.67	104.40	136.20	0.16
PBS 210	UNCON 2	2.580	36.9	381.78	305.30	198.50	0.46
PBS 209	UNCON 2	2.580	35.3	405.57	331.00	216.10	0.50
PBS 207	UNCON 2	2.580	41.0	434.78	328.13	257.60	0.49
PBS 206	UNCON 2	2.580	35.0	143.44	117.50	284.90	0.18
PBS 204	UNCON 2	2.580	42.2	606.77	449.50	354.60	0.67
PBS 203	UNCON 2	2.580	48.1	312.50	208.70	232.20	0.31



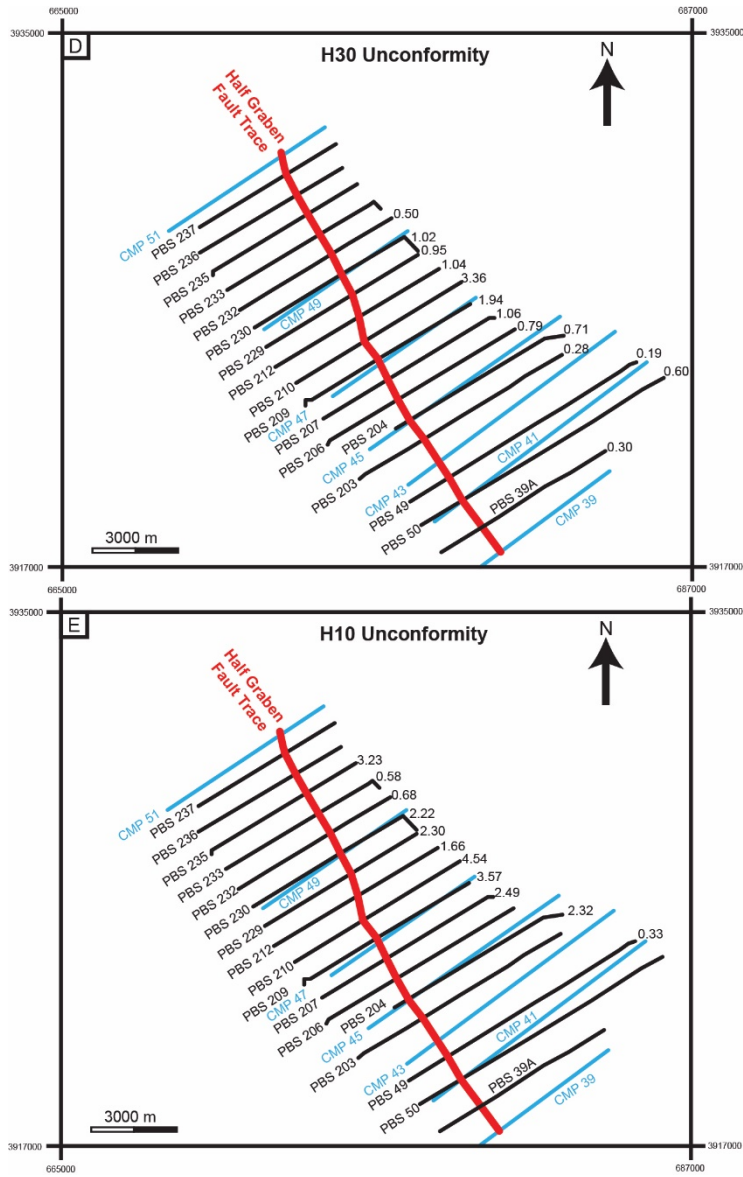


**Figure 3-1. Half Graben Fault Vector Map for all Seismic Lines That Were Evaluated in This Analysis. (A) Location of Each Seismic Line Used in This Analysis. Half Graben Fault Trace Compared to the Displacement Direction of the Hosgri Fault. (B) Each Seismic Line With its Corresponding Slip Rate in mm/yr for the UNCON 2 Unconformity. (C) Each Seismic Line With its Corresponding Slip Rate in Mm/Yr for the H40 East Unconformity. (D) Each Seismic Line With its Corresponding Slip Rate in mm/yr for the H30 Unconformity. (E) Each Seismic Line With its Corresponding Slip Rate in mm/yr for the H10 Unconformity.**

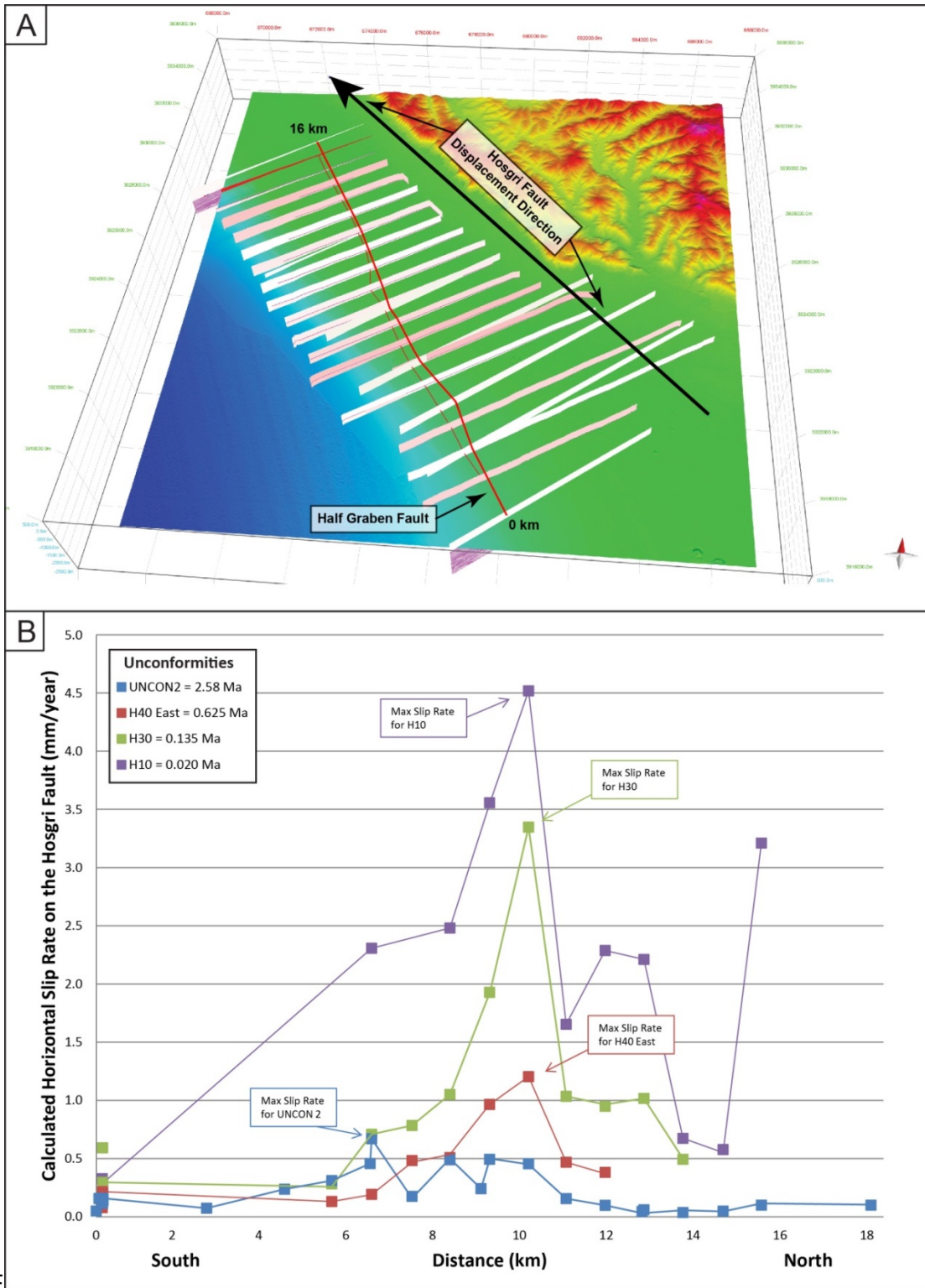


**Figure 3-2. Plot Showing Slip Rate for Each Seismic Line and Each Unconformity Versus Distance Along Half Graben Fault Trace With Respect to the Southernmost Line Used in This Analysis. Reference Map Shows the Location of Each Seismic Line Along the Trace of the Modeled Half Graben Fault. Base Map Is Seafloor Bathymetry.**

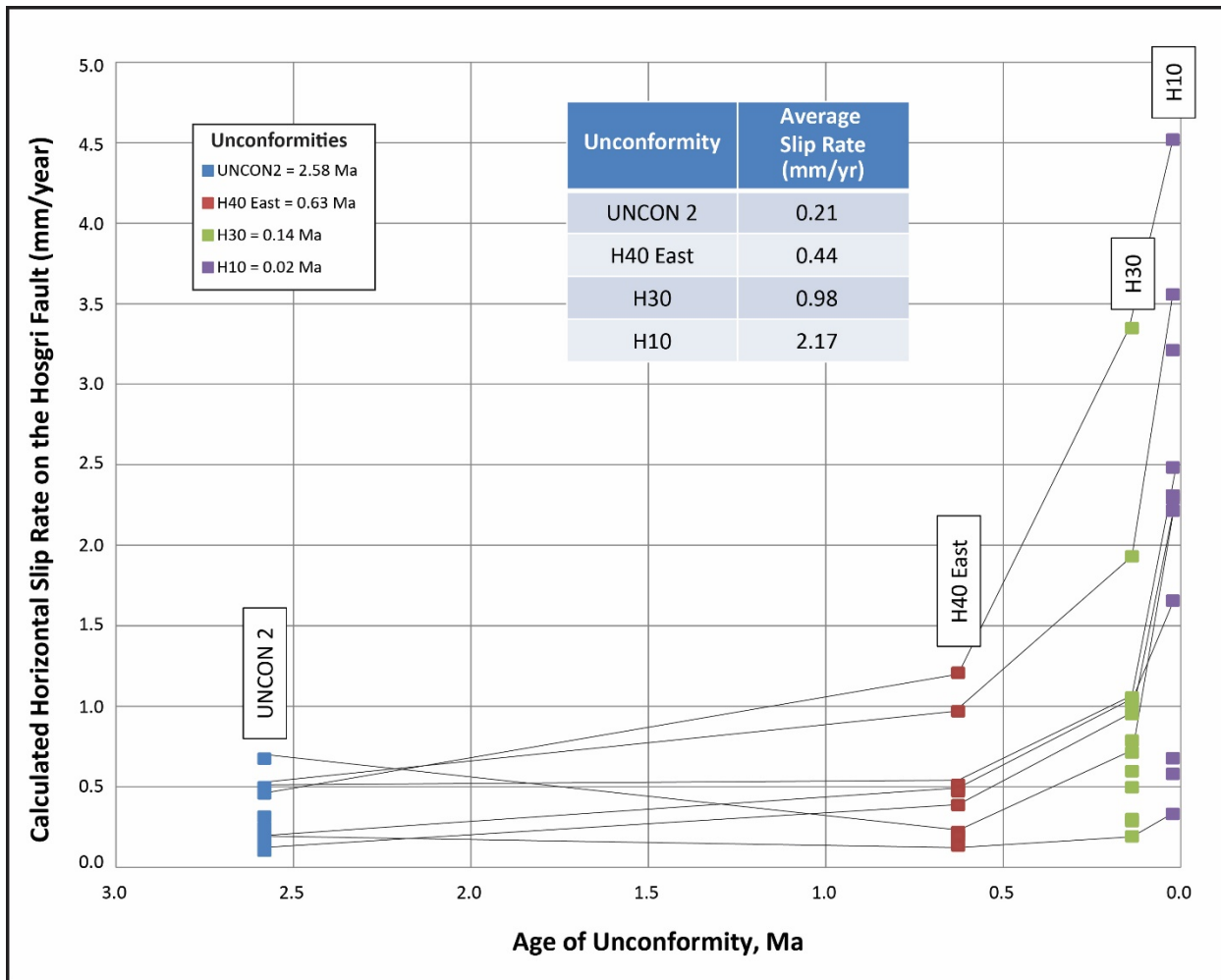


**Figure 3-3. Calculated Horizontal Slip Rate for the Hosgri Fault Over Time. Black Line Connects Each Slip Rate for Seismic Lines That Contain All Four Unconformities. Inset Shows Average Slip Rate for Each Unconformity.**

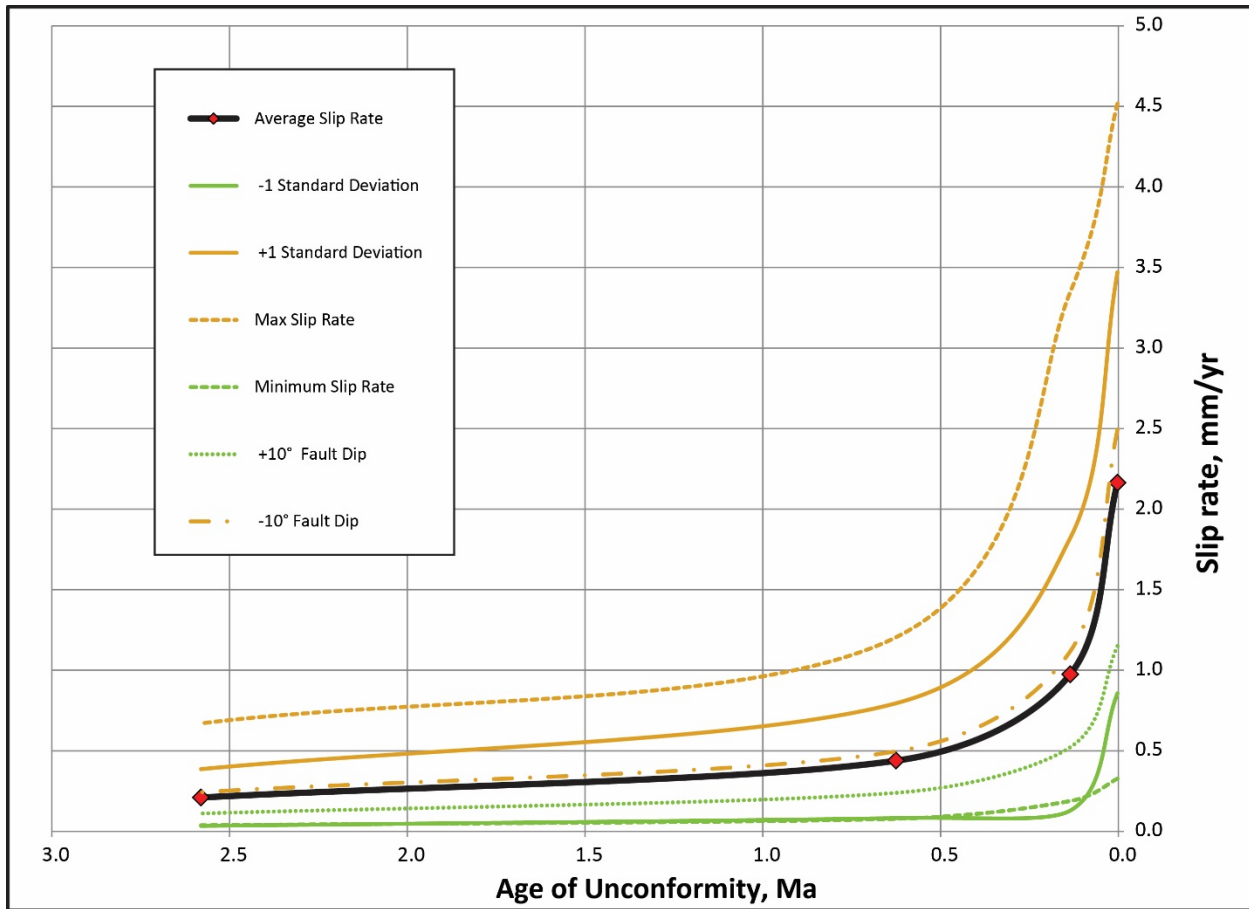


**Figure 3-4. Plot of Slip Rates Versus Age. Ages are Those of the Four Unconformities Used in the Analysis. The Average Values are Averages of the Slip Estimates From All of the Cross Sections Analyzed for a Given Unconformity. The +/- 1 Standard Deviation Bounds, and the Maximum and Minimum Bounds are Based on Variations in Slip Rate Estimates From Cross Section to Cross Section. The +10 Degree and -10 Degree Bounds are the Upper and Lower Bounds of the Ranges Derived From Using the "Best Fit" Fault Dip Values Compared With Slip Estimates Derived Using A +/- 10 Degrees of Fault Dip Range. Note That the Range of Slip Rate Estimates That Results From Varying the Fault Dip Lies Well Within the Variation Bounds of the "Raw" Measurements.**

## 4 DISCUSSION

Displacement profiles on faults tend to be complex with multiple maxima rather than simple profiles with a single displacement maximum. Strike-slip faults, like other fault types, grow by the linkage of multiple segments (e.g., de Jossineau and Aydin, 2009), and displacement tends to increase with fault length (Torabi and Berg, 2011). Some studies have shown that segments along a fault may rupture somewhat independently, with ruptures arrested short of the fault tip—for example at dilational jogs at segment boundaries—rather than rupturing the entire fault (e.g., Sibson, 1985). Consequently, significant variability in slip rate estimates should be expected within segmented strike-slip fault systems such as the Hosgri Fault zone.

The Hosgri fault is itself made up of multiple cooperating segments rather than a single fault surface. The Hosgri fault system is kinematically compatible—sharing general orientation and sense of slip—with other neighboring faults. For this analysis, the staff interprets the increasing slip rate in the Half Graben area as the result of increasing kinematic interaction and displacement transfer between the northwest end of the Hosgri fault and the southeast end of the San Simeon fault. The Half Graben is located near fault-tip defined displacement minima on the Hosgri and San Simeon faults. As kinematic cooperation (soft linkage) has developed, displacement rate has increased on the Half Graben fault. Theoretically, the Hosgri-San Simeon fault system may—over geologic time—become hard linked at the Earth's surface defined by a continuous surface rupture.

## 5 CONCLUSIONS

The Half Graben extensional basin is developed at a location where the displacement on the Hosgri fault to the south appears to be transferring to the San Simeon fault to the north. Horizontal displacement accommodated by the Half Graben fault represents a portion of the displacement on the Hosgri-San Simeon fault system. The Half Graben fault analysis was performed building on a single fault interpretation provided by Pacific Gas and Electric Company. The slip rates calculated at this location may not represent all the slip for the whole system because there may be multiple faults and distributed deformation accommodated by structures too small to image with seismic reflection data associated with the Half Graben structure. The results discussed in Section 3 show that the slip rates produced from this analysis based on four dated unconformities are below those used for the hazard assessment at Diablo Canyon Power Plant. The results show an increase in slip rate of 0.21 mm/yr for the oldest unconformity (UNCON2 = 2.58 Ma) to 2.17 mm/yr for the youngest unconformity (H10 = 0.02 Ma). With consideration of the uncertainties discussed in Section 2.5, the highest rate of 2.17 mm/yr is consistent with the rates PG&E is relying on in its 2015 PSHA (PG&E 2015b).

There are two alternative explanations for the apparent increase in slip rate. The increase in slip rates could simply represent an increase in activity on the Hosgri fault in the late Quaternary. Alternatively, the increase in slip rate could represent increasing cooperation and fault-linkage between the Hosgri and San Simeon faults. This latter alternative is a common feature of the evolution of interacting strike-slip faults. As the faults propagate laterally so that their fault tips overlap, overall fault displacement is distributed across the intervening transfer zone, in this case, the developing half-graben. Eventually the fault tips link, at which point the fault-system-parallel slip rate on the linking Half Graben fault will equal that of the whole strike-slip fault system at this location.

## 6 REFERENCES

- Argus, D.F. and R.G. Gordon. "Present Tectonic Motion Across the Coast Ranges and San Andreas Fault System in Central California." *Geological Society of America Bulletin*. Vol. 113, No. 12. pp.1,580–1,592. 2001.
- Atwater, T. "Plate Tectonic History of the Northeast Pacific and Western North America." E.L. Winterer, D.M. Hussong, and R.W. Decker, eds. "The Eastern Pacific Ocean and Hawaii." Boulder, Colorado: Geological Society of America. *The Geology of North America*. Vol. N. pp. 21–71. 1989.
- Burnham, K. "Predictive Model of San Andreas Fault System Paleogeography, Late Cretaceous to Early Miocene, Derived From Detailed Multidisciplinary Conglomerate Correlations." *Tectonophysics*. Vol. 464, Issues 1–4. pp.195–258. 2009.
- Clark, D.H., N.T. Hall, D.H. Hamilton, and R.G. Heck. "Structural Analysis of Late Neogene Deformation in the Central Offshore Santa Maria Basin." *Journal of Geophysical Research*. Vol. 96. pp. 6,435–6,458. 1991.
- de Jossineau, G. and A. Aydin. "Segmentation of Strike-Slip Faults Revisited." *Pure and Applied Geophysics*. Vol. 166. 1,575–1,594. 2009.
- DiSilvestro, L.A., K.L. Hanson, W.R. Lettis, and G.I. Shiller. "The San Simeon/Hosgri Pull-Apart Basin, South-Central Coastal California." *EOS Transactions of the American Geophysical Union*. Vol. 71, No. 43. 1,632 p. 1990.
- Dula, W.F., Jr. "Geometric Models of Listric Normal Faults and Rollover Folds." *American Association of Petroleum Geologist Bulletin*. Vol. 75. pp 1,609–1,625. 1991.
- Gawthrop, W. "The 1927 Lompoc, California Earthquake." *Bulletin of the Seismological Society of America*. Vol. 68, No. 6. pp 1,705–1,716. 1978.
- Gibbs, A.D. "Structural Evolution of Extensional Basins Margins." *Journal of the Geological Society of London*. Vol. 141. pp. 121–129. 1984.
- Gibbs, A.D. "Balanced Cross-Section Constriction From Seismic Sections in Areas of Extensional Tectonics." *Journal of Structural Geology*. Vol. 5, Issue 2. pp. 153–160. 1983.
- Hanson, K.L. and W.R. Lettis. "Estimated Pleistocene Slip Rate for the San Simeon Fault Zone, South Central Coastal California." I.B. Alterman, R.B. McMullen, L.S. Cluff, and D.B. Slemmons, eds. *Seismotectonics of the Central California Coast Ranges*. Geological Society of America Special Paper 292. pp. 133–150. 1994.
- Hanson, K.L., W.R. Lettis, M.K. McLaren, W.U. Savage, and N.T. Hall. "Style and Rate of Quaternary Deformation of the Hosgri Fault Zone." *Offshore South-Central California: U.S. Geological Survey Bulletin 1995-BB*. U.S. Geological Survey. pp. 1–33. 2004.
- Hardebeck, J.L. "Seismotectonics and Fault Structure of the California Central Coast." *Bulletin Seismological Society of America*. Vol. 100. pp 1,031–1,050. 2010.

- Hornafius, J.S., B.P. Luyendyk, R.R. Terres, and M.J. Kamerling. "Timing and Extent of Neogene Tectonic Rotation in the Western Transverse Ranges, California." *Geological Society of America Bulletin*. Vol. 97. pp. 1,476–1,478. 1986.
- Hoskins, E. and J. Griffiths. "Hydrocarbon Potential of Northern and Central California Offshore: Region 2." AAPG. Special Volume, A128. pp. 212–228. 1971.
- Johnson, S.Y. and J.T. Watt. "Influence of Fault Trend, Bends, and Convergence on Shallow Structure and Geomorphology of the Hosgri Strike-Slip Fault, Offshore Central California." *Geosphere*. Vol. 8. pp. 1,632–1,656. 2012.
- Johnson, S.Y., S.R. Hartwell, and P. Dartnell. "Offset of Latest Pleistocene Shoreface Reveals Slip Rate on the Hosgri Strike-Slip Fault, Offshore Central California." *Bulletin of the Seismological Society of America*. Vol. 104. doi:10.1785/012013057. 2014.
- Kluesner, J.W. and D.S. Brothers. "Seismic Attribute Detection of Faults and Fluid Pathways Within an Active Strike-Slip Shear Zone: New Insights Form High-Resolution 3D P-Cable™ Seismic Data Along the Hosgri Fault, Offshore California." *Interpretation*. Vol. 4. pp. SB131–SB148. 2016.
- Lettis, W.R. and K.L. Hanson. "Crustal Strain Partitioning; Implications for Seismic Hazard Assessment in Western California." *Geology*. Vol. 19. pp. 559–562. 1992.
- Lettis, W.R., K.L. Hanson, J.R. Unruh, M. McLaren, and W.U. Savage. "Quaternary Tectonic Setting of South-Central Coastal California." M.A. Keller, ed. *Evolution of Sedimentary Basins/Offshore Oil and Gas Investigations—Santa Maria Province*, Bulletin 1995. Chapter AA, U.S. Geological Survey. 24p. 2004.
- Lettis, W.R., K.I. Kelson, J.R. Wesling, M. Angell, K.L. Hanson, and N.T. Hall. "Quaternary Deformation of the San Luis Range, San Luis Obispo County, California." I.B. Alterman, R.B. McMullen, L.S. Cluff, and D.B. Slemmons, eds. *Seismotectonics of the Central California Coast Ranges*. Geological Society of America Special Paper 292. pp. 111–132. 1994.
- Lettis, W.R., L. DiSilvestro, K.L. Hanson, and G.I. Shiller. "The San Simeon/Hosgri Pull-Apart Basin; Implications for Late Quaternary Activity on the Hosgri Fault Zone." W.R. Lettis, K.L. Hanson, K.I. Kelson, and J.R. Wesling, eds. *Neotectonics of the South-Central Coastal California: Friends of the Pleistocene*. Pacific Cell. 1990 Fall Field Trip Guidebook. pp. 91–138. 1990.
- McLaren, M.K. and W.U. Savage. "Seismicity of South-Central Coastal California: October 1987 through January 1997." *Bulletin of the Seismological Society of America*. Vol. 91 Issue 6. pp. 1,629–1,658. 2001.
- McLaren, M.K., J.L. Hardebeck, N. van der Elst, J.R. Unruh, G.W. Bawden, and J.L. Blair. "Complex Faulting Associated With the 22 December 2003 M-w 6.5 San Simeon, California, Earthquake, Aftershocks, and Postseismic Surface Deformation." *Bulletin of the Seismological Society of America*. Vol. 98. pp. 1,659–1,680. 2008.

PG&E. "Seismic Source Characterization for Probabilistic Seismic Hazard Analysis for the Diablo Canyon Power Plant, San Luis Obispo County, California." Report on the Results of the SSHAC Level 3 Study in Partial Compliance with NRC Letter 50.54(f), dated March 2015. 2015a

\_\_\_\_\_. "Response to NRC Request for Information Pursuant to 10 CFR 50.54(f) Regarding the Seismic Aspects of Recommendation 2.1 of the Near-Term Task Force Review from the Fukushima Dai-ichi Accident." Seismic Hazard and Screening Report, dated March 11, 2015. 2015b

\_\_\_\_\_. "Offshore Low-Energy Seismic Reflection Studies in Estero Bay, San Luis Obispo Bay, and Point Sal Areas." PG&E Technical Report, GEO.DCPP.TR.14.02. Pacific Gas and Electric Company. 2014.

\_\_\_\_\_. "Stratigraphic Framework for Assessment of Fault Activity Offshore of the Central California Coast Between Point San Simeon and Point Sal." PG&E Technical Report GEO.DCPP.TR.13.01. Pacific Gas and Electric Company. 76p. 2013.

\_\_\_\_\_. "Addendum to the 1988 Final Report of the Diablo Canyon Long Term Seismic Program." U.S. Nuclear Regulatory Commission Docket No. 50-275 and No. 50-323. Pacific Gas and Electric Company. February 1991.

\_\_\_\_\_. "Final Report of the Diablo Canyon Long Term Seismic Program, U.S. Nuclear Regulatory Commission Docket Nos. 50-275 and 50-323." Pacific Gas and Electric Company. 1988.

Rahe, B., D.A. Ferrill, and A.P. Morris. "Physical Analog Modeling of Pull-Apart Basin Evolution." *Tectonophysics*. Vol. 285, Issue 1–2. pp. 21–40. 1998.

Rosendahl, B.R., D. Reynolds, P. Lorber, C. Burgess, J. McGill, D. Scott, J. Lambiase, and S. Derksen. "Structural Expressions of Rifting: Lessons From Lake Tanganyika." L.E. Frostick, et al., ed. Sedimentation in the East African Rifts. *Geological Society of London Special Publication*. Vol. 25. pp. 29–43. 1986.

Rowland, J.V. and R.H. Sibson. "Extensional Fault Kinematics Within the Taupo Volcanic Zone, New Zealand: Soft-Linked Segmentation of a Continental Rift System." *New Zealand Journal of Geology and Geophysics*. Vol. 44, Issue 2. pp. 271–283. 2001.

Rowan, M.G. and R. Kligfield. "Cross Section Restoration and Balancing as an Aid to Seismic Interpretation in Extensional Terranes." *American Association of Petroleum Geologists Bulletin*. Vol. 73. pp. 955–966. 1989.

Sibson, R. "Stopping of Earthquake Ruptures at Dilational Fault Jogs." *Nature*. Vol. 316. pp 248–251. 1985.

Sorlien, C.C., M.J. Kamerling, and D. Mayerson. "Block Rotation and Termination of the Hosgri Strike-Slip Fault, California, From Three-Dimensional Map Restoration." *Geology*. Vol. 27, No 11. pp. 1,039–1,042. 1999.

Steritz, J.W. and B.P. Luyendyk. "Hosgri Fault Zone, Offshore Santa Maria Basin, California." I.B. Alterman, R.B. McMullen, L.S. Cluff, D.B. and Slemmons, eds. *Seismotectonics of the Central California Coast Ranges*. Geological Society of America Special Paper 292. pp. 191–209. 1994.

Torabi, A. and S. S. Berg. "Scaling of Fault Attributes: A Review." *Marine and Petroleum Geology*. Vol. 28 Issue 8. pp. 1,444–1,460. 2011.

Verrall, P. *Structural interpretation with applications to north sea problems*. Course Notes. No. 3. Joint Association for Petroleum Exploration Courses (U.K.). 1981.

White, N.J., J.A. Jackson, and D.P. McKenzie. "The Relationship Between the Geometry of Normal Faults and That of the Sedimentary Layers in Their Hanging Walls." *Journal of Structural Geology*. Vol. 8, Issue 8. pp. 897–909. 1986.

Willingham, C.R., J.D. Rietman, R.G. Heck, and W.R. Lettis. "Characterization of the Hosgri Fault Zone and Adjacent Structures in the Offshore Santa Maria Basin, South Central California." M.A. Keller, ed. *Evolution of Sedimentary Basins/Onshore Oil and Gas Investigations—Santa Maria Province*. U.S. Geological Survey Bulletin 1995-CC. 105p. 2013.

Zeng, Y. and Z-K. Shen. "Fault Network Modeling of Crustal Deformation in California Constrained Using GPS and Geologic Observations." *Tectonophysics*. Vols. 612–613. pp. 1–17. 2014.